JOC Article

Control of Peptide Helix Sense by Temperature Tuning of Noncovalent Chiral Domino Effect

Hisatoshi Komori and Yoshihito Inai*

Department of Environmental Technology and Urban Planning, Shikumi College, Graduate School of Engineering, Nagoya Institute of Technology, Gokiso-cho, Showa-ku, Nagoya 466-8555, Japan

inai.yoshihito@nitech.ac.jp

Received December 11, 2006

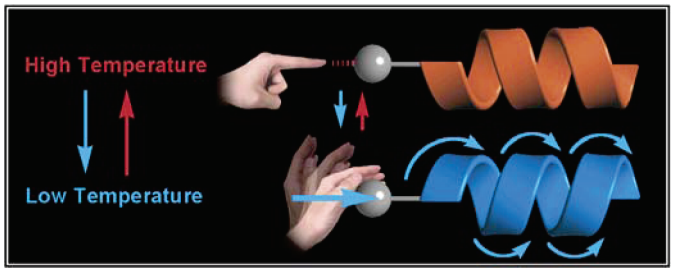

We have investigated temperature effect on control of a peptide helix sense through the noncovalent chiral domino effect (NCDE: Inai, Y. et al., *J. Am. Chem. Soc.* **2003**, *125*, 8151−8162). Nonapeptide (**1**: Inai, Y.; Komori, H. *Biomacromolecules* **2004**, *5*, 1231−1240), which alone prefers a right-handed helix, maintained a screw-sense balance or a small imbalance at room temperature in the presence of Boc-D-amino acid. Cooling of the solution induced a left-handed helix more clearly. Conversely, heating from room temperature recovered the original right-handed sense. This helix−helix transition was essentially reversible in cooling−heating cycles. An increase in the Boc-D-amino acid concentration elevated temperature for switching CD signs based on the conformational transition. A similar thermal-driven inversion of helix sense was observed for **1** at other initial concentrations, suggesting that this behavior is insensitive to some peptide aggregation. NMR study provided direct evidence for the domino-type control of helix sense, in which Boc-Leu-OH is mainly located at the N-terminal segment. In addition, a left-handed helix induced by the D-isomer was shown to participate in equilibrium with a right-handed helix, whereas the right-handed helix was predominant in the presence of L-isomer. Consequently, we here have proposed a model for controlling a peptide helix sense (or its screw-sense bias) through temperature tuning of the external chiral interaction specific to the N-terminal sequence.

Introduction

Thermal-driven control of a polymer helicity not only demonstrates significant phenomena for understanding the dynamic origin of a biological one-handed helix, but also offers us unique functional potentials relevant to molecular switches.[1−4] Such intriguing phenomena have indeed been achieved in several chiral backbones of artificial and bio-related polymers.[2,3] The temperature dependence of helicity basically arises from the thermodynamic nature of a helical chain itself.[2,3] In most cases, thermal driving force for the helix−helix transition has been essentially used as nonsite specific stimuli to a whole helical backbone.

(1) For comprehensive reviews for helical polymers, see: (a) Hill, D. J.; Mio, M. J.; Prince, R. B.; Hughes, T. S.; Moore, J. S. *Chem. Rev.* **2001**, *101*, 3893−4011. (b) Nakano, T.; Okamoto, Y. *Chem. Rev.* **2001**, *101*, 4013−4038. (c) Cornelissen, J. J. L. M.; Rowan, A. E.; Nolte, R. J. M.; Sommerdijk, N. A. J. M. *Chem. Rev.* **2001**, *101*, 4039−4070. (d) Green, M. M.; Park, J.-W.; Sato, T.; Teramoto, A.; Lifson, S.; Selinger, R. L. B.; Selinger, J. V. *Angew. Chem., Int. Ed.* **1999**, *38*, 3138−3154. (e) Brunsveld, L.; Folmer, B. J. B.; Meijer, E. W.; Sijbesma, R. P. *Chem. Rev.* **2001**, *101*, 4071−4097.

(2) For leading examples of thermal-driven control of helicity in artificial polymers, see: (a) Cheon, K. S.; Selinger, J. V.; Green, M. M. *Angew. Chem., Int. Ed.* **2000**, *39*, 1482−1485. (b) Tang, K.; Green, M. M.; Cheon, K. S.; Selinger, J. V.; Garetz, B. A. *J. Am. Chem. Soc.* **2003**, *125*, 7313−7323. (c) Tang, H.-Z.; Boyle, P. D.; Novak, B. M. *J. Am. Chem. Soc.* **2005**, *127*, 2136−2142. (d) Fujiki, M. *J. Am. Chem. Soc.* **2000**, *122*, 3336−3343. (e) Fujiki, M. *Macromol. Rapid Commun.* **2001**, *22*, 539−563. (f) Teramoto, A.; Terao, K.; Terao, Y.; Nakamura, N.; Sato, T.; Fujiki, M. *J. Am. Chem. Soc.* **2001**, *123*, 12303−12310. (g) Koe, J. R.; Fujiki, M.; Nakashima, H.; Motonaga, M. *Chem. Commun.* **2000**, 389−390. (h) Kim, S.-Y.; Fujiki, M.; Ohira, A.; Kwak, G.; Kawakami, Y. *Macromolecules* **2004**, *37*, 4321−4324. (i) Tabei, J.; Nomura, R.; Sanda, F.; Masuda, T. *Macromolecules* **2004**, *37*, 1175−1179. (j) Nakako, H.; Nomura, R.; Masuda, T. *Macromolecules* **2001**, *34*, 1496−1502. (k) Tabei, J.; Nomura, R.; Masuda, T. *Macromolecules* **2003**, *36*, 573−577. For folding processes of unique oligomeric backbones, see: (l) Prince, R. B.; Brunsveld, L.; Meijer, E. W.; Moore, J. S. *Angew. Chem., Int. Ed.* **2000**, *39*, 228−230. (m) Nelson, J. C.; Saven, J. G.; Moore, J. S.; Wolynes, P. G. *Science* **1997**, *277*, 1793−1796.

10.1021/jo0625305 CCC: $37.00
Published on Web 04/28/2007

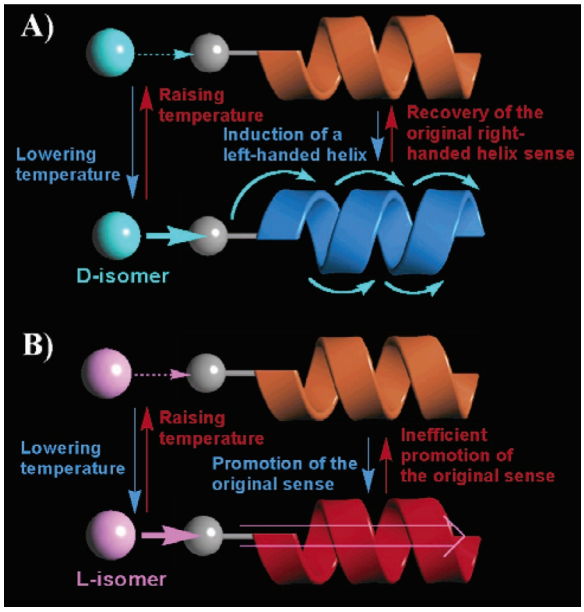

FIGURE 1. Conceptual model for control of a helix sense through the temperature tuning of an external chiral power that is essentially specific to one terminus of a target peptide. Temperature effects modulate interaction of (A) D-molecule or (B) L-molecule with the peptide favoring a right-handed helix. For the basic concept of the NCDE, see refs 5−7. The graphics were mainly made in ref 8.

We here propose a model for controlling a peptide helix sense by *temperature stimuli specific to its chain end*. The temperature effects are mainly used for tuning external chiral power that governs the whole screw sense, rather than for modulating thermodynamic parameters of the two helical forms. Our group has reported control of a screw sense of 3_{10}-helical peptide through an external chiral molecule.[5−7] Here, free NH groups in the N-terminal helical sequence bind the chiral molecule to form a dynamic complex. Asymmetry of the terminal complex influences the whole helix sense (this phenomenon is figuratively termed "noncovalent chiral domino effect (NCDE)").[5−7] At this point, temperature effect might modulate the noncovalent interaction for the complex formation. Consequently, the chiral power is possibly strengthened by lowering the temperature, while the chiral power is weakened by raising the temperature. The thermally tunable chiral effect thus might promise temperature control of the whole helix sense, as proposed in Figure 1.

To demonstrate the model, we here have adopted a combination of nonapeptide (**1**) versus chiral acid.[7]

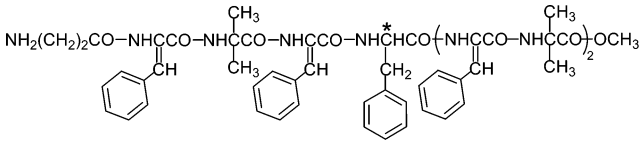

H-β-Ala-Δ^ZPhe-Aib-Δ^ZPhe-L-Phe-(Δ^ZPhe-Aib)$_2$-OCH$_3$

(**1**: β-Ala = β-alanine; Δ^ZPhe = *Z*-α,β-dehydrophenylalanine; Aib = α-aminoisobutyric acid; Phe = phenylalanine)[7]

We already demonstrated control of the original helicity through external chiral stimulus at room temperature.[7] That is, peptide **1**, composed primarily of achiral, helix-forming Δ^ZPhe and Aib residues,[9] adopts a right-handed 3_{10}-helix due to the single, internal L-residue.[7,10−17] The original helicity is influenced by the addition of chiral Boc-amino acid (Boc = *t*-butoxycarbonyl), depending on its chiral sign, amino-acid type, and concentration. Regarding the chiral sign, the original helicity is promoted by the L-isomer, but is reduced by the D-isomer.[7] In a more effective case, increasing the concentration of Boc-D-amino acid gives rise to a left-handed helix via a screw-sense balance.[7]

We here have carried out CD and NMR measurements of peptide **1** with chiral Boc-amino acid at several temperatures.

(3) For bio-related polymers undergoing helix−helix transition, see: (a) Ushiyama, A.; Furuya, H.; Abe, A.; Yamazaki, T. *Polym. J.* **2002**, *34*, 450−454. (b) Watanabe, J.; Okamoto, S.; Satoh, K.; Sakajiri, K.; Furuya, H.; Abe, A. *Macromolecules* **1996**, *29*, 7084−7088. (c) Watanabe, J.; Okamoto, S.; Abe, A. *Liq. Cryst.* **1993**, *15*, 259−263. (d) Tsujita, Y. *Biol. Chem.* **1988**, *31*, 11−20. (e) Tsujita, Y.; Ojika, R.; Tsuzuki, K.; Takizawa, A.; Kinoshita, T. *J. Polym. Sci., Part A: Polym. Chem.* **1987**, *25*, 1041−1048. (f) Toriumi, H.; Saso, N.; Yasumoto, Y.; Sasaki, S.; Uematsu, I. *Polym. J.* **1979**, *11*, 977−981. (g) Ueno, A.; Nakamura, J.; Adachi, K.; Osa, T. *Makromol. Chem., Rapid Commun.* **1989**, *10*, 683−686. (h) Wolf, F. A.; Keller, R. C. A. *Prog. Colloid Polym. Sci.* **1996**, *102*, 9−14. (i) Sakajiri, K.; Satoh, K.; Kawauchi, S.; Watanabe, J. *J. Mol. Struct.* **1999**, *476*, 1−8. (j) Tashiro, R.; Sugiyama, H. *J. Am. Chem. Soc.* **2005**, *127*, 2094−2097. (k) Chaires, J. B.; Sturtevant, J. M. *Biopolymers* **1988**, *27*, 1375−1387. (l) Thomas, G. A.; Peticolas, W. L. *Biopolymers* **1989**, *28*, 1625−1636.

(4) For reviews of "molecular switches" or "chiroptical switches", see: (a) Feringa, B. L.; van Delden, R. A.; Koumura, N.; Geertsema, E. M. *Chem. Rev.* **2000**, *100*, 1789−1816. (b) Feringa, B. L. *Acc. Chem. Res.* **2001**, *34*, 504−513. (c) Stoddart, J. F. *Acc. Chem. Res.* **2001**, *34*, 410−411. (d) Balzani, V.; Credi, A.; Raymo, F. M.; Stoddart, J. F. *Angew. Chem., Int. Ed.* **2000**, *39*, 3348−3391. (e) Harada, A. *Acc. Chem. Res.* **2001**, *34*, 456−464. (f) Pieroni, O.; Fissi, A.; Angelini, N.; Lenci, F. *Acc. Chem. Res.* **2001**, *34*, 9−17. For chiral switch using bio-related components, refs 3k,4j; see also: (g) Asakawa, M.; Brancato, G.; Fanti, M.; Leigh, D. A.; Shimizu, T.; Slawin, A. M. Z.; Wong, J. K. Y.; Zerbetto, F.; Zhang, S. *J. Am. Chem. Soc.* **2002**, *124*, 2939−2950. (h) Ueno, A.; Takahashi, K.; Anzai, J.; Osa, T. *J. Am. Chem. Soc.* **1981**, *103*, 6410−6415. Unique artificial backbones undergoing ligand-mediated switching were found: (i) Barboiu, M.; Lehn, J.-M. *Proc. Natl. Acad. Sci. U.S.A.* **2002**, *99*, 5201−5206. (j) Barboiu, M.; Vaughan, G.; Kyritsakas, N.; Lehn, J.-M. *Chem. Eur. J.* **2003**, *9*, 763−769.

(5) (a) Inai, Y.; Tagawa, K.; Takasu, A.; Hirabayashi, T.; Oshikawa, T.; Yamashita, M. *J. Am. Chem. Soc.* **2000**, *122*, 11731−11732. (b) Inai, Y. In *Recent Research Developments in Macromolecules*; Pandalai, S. G., Ed.; Research Signpost: Trivandrum, India, 2002; Chapter 2, pp 37−57. (c) Inai, Y.; Hirano, T. *ITE Lett. Batteries, New Technol. Med.* **2003**, *4*, 485−488. (d) Inai, Y.; Komori, H.; Takasu, A.; Hirabayashi, T. *Biomacromolecules* **2003**, *4*, 122−128. (e) Inai, Y.; Ishida, Y.; Tagawa, K.; Takasu, A.; Hirabayashi, T. *J. Am. Chem. Soc.* **2002**, *124*, 2466−2473.

(6) (a) Inai, Y.; Ousaka, N.; Okabe, T. *J. Am. Chem. Soc.* **2003**, *125*, 8151−8162. (b) Inai, Y.; Ousaka, N.; Ookouchi, Y. *Biopolymers* **2006**, *82*, 471−481. (c) Ousaka, N.; Inai, Y.; Okabe, T. *Biopolymers* **2006**, *83*, 337−351.

(7) Inai, Y.; Komori, H. *Biomacromolecules* **2004**, *5*, 1231−1240.

(8) Figure 1 and the Table of Content graphic were drawn partially with the software "ArgusLab": Thompson, M. A. *ArgusLab 4.0.1*; Planaria Software LLC: Seattle, WA, 2004 (http://www.arguslab.com).

(9) For the helical chains containing Aib or Δ^ZPhe residues, see: (a) Karle, I. L.; Gopi, H. N.; Balaram, P. *Proc. Natl. Acad. Sci. U.S.A.* **2003**, *100*, 13946−13951. (b) Venkatraman, J.; Shan-karamma, S. C.; Balaram, P. *Chem. Rev.* **2001**, *101*, 3131−3152. (c) Karle, I. L.; Flippen-Anderson, J. L.; Uma, K.; Balaram, H.; Balaram, P. *Proc. Natl. Acad. Sci. U.S.A.* **1989**, *86*, 765−769. (d) Benedetti, E.; Bavoso, A.; Di Blasio, B.; Pavone, V.; Pedone, C.; Crisma, M.; Bonora, G. M.; Toniolo, C. *J. Am. Chem. Soc.* **1982**, *104*, 2437−2444. (e) Toniolo, C.; Benedetti, E. *Trends Biochem. Sci.* **1991**, *16*, 350−353. (f) Okuyama, K.; Saga, Y.; Nakayama, M.; Narita, M. *Biopolymers* **1991**, *31*, 975−85. (g) Yanagisawa, K.; Morita, T.; Kimura, S. *J. Am. Chem. Soc.* **2004**, *126*, 12780−12781. (h) Rajashankar, K. R.; Ramakumar, S.; Chauhan, V. S. *J. Am. Chem. Soc.* **1992**, *114*, 9225−9226. (i) Jain, R. M.; Rajashankar, K. R.; Ramakumar, S.; Chauhan, V. S. *J. Am. Chem. Soc.* **1997**, *119*, 3205−3211. (j) Ramagopal, U. A.; Ramakumar, S.; Sahal, D.; Chauhan, V. S. *Proc. Natl. Acad. Sci. U.S.A.* **2001**, *98*, 870−874. (k) Ciajolo, M. R.; Tuzi, A.; Pratesi, C. R.; Fissi, A.; Pieroni, O. *Biopolymers* **1990**, *30*, 911−920. (l) Ciajolo, M. R.; Tuzi, A.; Pratesi, C. R.; Fissi, A.; Pieroni, O. *Biopolymers* **1992**, *32*, 717−724. (m) Mitra, S. N.; Dey, S.; Karthikeyan, S.; Singh, T. P. *Biopolymers* **1997**, *41*, 97−105. (n) Chauhan, V. S.; Uma, K.; Kaur, P.; Balaram, P. *Biopolymers* **1989**, *28*, 763−771. Similar references are also given in ref 6.

The results obtained support the model shown in Figure 1. That is, the helix sense can be controlled (promoted, reduced, or inverted) by thermal tuning of the external chiral power. The present findings also imply that noncovalent interaction at the N-terminus of a helical peptide plays a critical role in its structural stability. Moreover, this basic knowledge should be applied to the design of peptide-based "chiroptical switches"[4] in which the molecular asymmetry is manipulated by the terminal-specific inputs, such as chiral stimulus and temperature.

Results and Discussion

Temperature Effect on the Helicity of Peptide 1 Alone. First of all, variable-temperature CD measurement was carried out for a chloroform solution of **1** without chiral additive. Figure 2 shows the temperature change of the CD spectra.

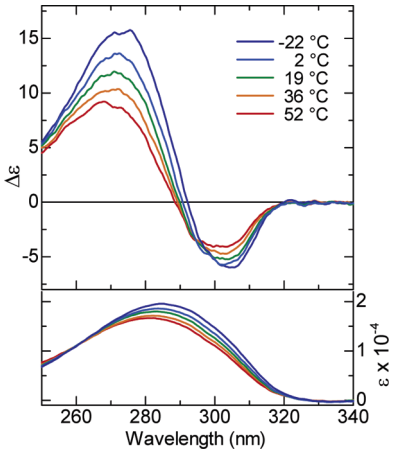

FIGURE 2. CD (upper) and UV absorption spectra of peptide **1** alone in chloroform at temperatures ranging from −22 to 52 °C. The $\Delta\epsilon$ and ϵ are expressed per a Δ^ZPhe unit.

Peptide **1** at room temperature (ca. 19 °C), as previously reported,[7,12c] yielded a split-type CD pattern around 283 nm of the Δ^ZPhe chromophore. The pattern is characterized by couplets of a negative peak at a longer wavelength to a positive peak (− to +). Identification of the helix sense from the split-CD sign has also been established for Δ^ZPhe-containing peptides.[6,7,12,18,19] Here, the sign of (− to +) corresponds to a right-handed 3_{10}-helix in alternating sequences $-(\Delta^Z\text{Phe-X})_n-$.[6] We also simulated the theoretical electronic CD spectra of peptide **1** in helical conformations.[12c] A split CD pattern of (− to +) can be produced by a right-handed 3_{10}-helix carrying Δ^ZPhe's phenyl groups essentially in a vertical orientation, while the opposite CD pattern is obtained by a left-handed 3_{10}-helix.[12c]

The heating and cooling processes from room temperature do not influence the starting CD pattern, suggesting that the original right-handed sense remains thermally unchanged. Meanwhile, the CD amplitudes as well as the corresponding absorption intensities were somewhat enhanced by decreasing temperature. The CD-signal promotion should be interpreted as reasonable phenomena, where thermal structural fluctuations leading to the reduction of CD intensities are more restricted at lower temperatures.[20] The corresponding absorption band slightly shifted to about 284.6 nm (−22 °C) from about 283.2 nm (19 °C). However, peptide **1** alone shows no clear tendency to undergo helix inversion in this range.

Temperature-Induced Control of the Helix Sense of Peptide 1 with Boc-D-Amino Acid. Next we have investigated temperature effects on CD spectra of **1** in the presence of Boc-D-Pro-OH. The D-additive at a moderate amount (1 mM) yielded

(10) The present study needs a molecular system in which external stimulus governs the helix sense of a chiral peptide. In this regard, the β-Ala N-terminus receives the external chiral stimulus more effectively, compared with α-residual N-terminus.[6a,c] (Chain flexibility of the β-Ala might facilitate to bind chiral molecule. For β-Ala conformations, see also ref 11). In sequence **1**, the Δ^ZPhe and Aib residues are employed for promotion of a helical structure.[13] In addition, the Δ^ZPhe residue produces a solvent- or additive-free absorption band around 280 nm,[6,7,12] at which CD analysis can highlight the chiral information of peptide **1** itself. The helical structure of peptide **1** was clarified by NMR and IR spectroscopy and conformational energy computation.[7] The presence of a 3_{10}-helix[13] was supported from solvent dependence on NH chemical shifts[6,7,9i,n,14]: the Δ^ZPhe(4) to Aib(9) NH's resonances were essentially shielded from solvent, whereas the Aib(3) NH was more sensitive to solvent composition.[7] These solvent-shielded NHs correspond to the intramolecular hydrogen-bonding pattern characteristic of a 3_{10}-helix.[6,7,9i,n] Energy minimization from a 3_{10}-helical conformation maintains a 3_{10}-helix essentially.[7] Moreover, such 3_{10}-helix was found in the crystalline structure of analogous Boc-(Aib-Δ^ZPhe)$_4$-Aib-OCH_3.[15] Furthermore, temperature dependence of NMR spectra[16] has been investigated for peptide **1** in $CDCl_3$ in Figure S8. Here the temperature coefficient (−ppb/*K*) of each NH proton was estimated from the NMR data at 293−278 K (or at 293−273 K): 1.8x10 (2.0x10) for Aib(3); 6.9 (9.0) for Δ^ZPhe(4); 1.2 (1.4) for Phe(5); 4.9 (6.0) for Δ^ZPhe(6); 0.4 (0.5) for Aib(7); 3.3 (3.3) for Δ^ZPhe(8); 2.3 (2.0) for Aib(9). As a result, the Aib(3) NH showed the largest value among the seven amide NH's clearly detected at room temperature. This tendency agrees with the solvent-dependent NH pattern.[7] Meanwhile, relatively large values were seen in the Δ^ZPhe(4) and Δ^ZPhe(6) NH's, whereas these two protons were shown to be essentially insensitive to the solvent composition.[7] A relatively large coefficient of Δ^ZPhe(4) NH might imply that a 3_{10}-helix of peptide **1** fluctuates dynamically or contains an α-helical moiety as a minority.[17]

(11) (a) Cheng, R. P.; Gellman, S. H.; DeGrado, W. F. *Chem. Rev.* **2001**, *101*, 3219−3232. For similar peptide design of β-Ala's N-terminus for high binding affinity, refs 6a,c; see also, (b) Banerjee, A.; Maji, S. K.; Drew, M. G. B.; Haldar, D.; Banerjee, A. *Tetrahedron Lett.* **2003**, *44*, 699−702.

(12) For comprehensive CD and UV absorption studies of Δ^ZPhe-containing peptides, see: (a) Pieroni, O.; Fissi, A.; Jain, R. M.; Chauhan, V. S. *Biopolymers* **1996**, *38*, 97−108. (b) Pieroni, O.; Montagnoli, G.; Fissi, A.; Merlino, S.; Ciardelli, F. *J. Am. Chem. Soc.* **1975**, *97*, 6820−6826. For simulation of CD spectra of peptide **1** in helical conformations, see: (c) Komori, H.; Inai, Y. *J. Phys. Chem. A* **2006**, *110*, 9099−9107.

(13) For summary of 3_{10}-helical structures, see refs 9b,e.

(14) Pitner, T. P.; Urry, D. W. *J. Am. Chem. Soc.* **1972**, *94*, 1399−1400.

(15) Inai, Y.; Oshikawa, T.; Yamashita, M.; Tagawa, K.; Hirabayashi, T. *Biopolymers* **2003**, *70*, 310−322.

(16) For the relation between temperature coefficient of NH and intramolecular hydrogen bond, see: (a) Andersen, N. H.; Neidigh, J. W.; Harris, S. M.; Lee, G. M.; Liu, Z.; Tong, H. *J. Am. Chem. Soc.* **1997**, *119*, 8547−8561. (b) Baxter, N. J.; Williamson, M. P. *J. Biomol. NMR* **1997**, *9*, 359−369. (c) Stevens, E. S.; Sugawara, N.; Bonora, G. M.; Toniolo, C. *J. Am. Chem. Soc.* **1980**, *102*, 7048−7050.

(17) Transition between 3_{10}-helix and α-helix, or occurrence of the 3_{10}-/α-mixed helices have already been reported[9c,17a−e]: (a) Crisma, M.; Bisson, W.; Formaggio, F.; Broxterman, Q. B.; Toniolo, C. *Biopolymers* **2002**, *64*, 236−245. (b) Lazo, N. D.; Downing, D. T. *J. Biol. Chem.* **1999**, *274*, 37340−37344. (c) Fiori, W. R.; Miick, S. M.; Millhauser, G. L. *Biochemistry* **1993**, *32*, 11957−11962. (d) Smythe, M. L.; Huston, S. E.; Marshall, G. R. *J. Am. Chem. Soc.* **1995**, *117*, 5445−5452. (e) Millhauser, G. L.; Stenland, C. J.; Hanson, P.; Bolin, K. A.; van de Ven, F. J. M. *J. Mol. Biol.* **1997**, *267*, 963−974.

(18) For the exciton chirality method for absolute assignment of chiral sign, see: (a) Harada, N.; Chen, S.-M. L.; Nakanishi, K. *J. Am. Chem. Soc.* **1975**, *97*, 5345−5352. (b) Harada, N.; Nakanishi, K. *Circular Dichroic Spectroscopy. Exciton Coupling in Organic Stereochemistry*; University Science Books: Mill Valley, CA, 1983. For theoretical CD calculations that are elegantly performed for helical polypeptides, see: (c) Woody, R. W.; Koslowski, A. *Biophys. Chem.* **2002**, *101*−*102*, 535−551. (d) Manning, M. C.; Woody, R. W. *Biopolymers* **1991**, *31*, 569−586. (e) Sisido, M.; Egusa, S.; Imanishi, Y. *J. Am. Chem. Soc.* **1983**, *105*, 1041−1049. (f) Sisido, M.; Ishikawa, Y.; Harada, M.; Itoh, K. *Macromolecules* **1991**, *24*, 3999−4003.

(19) In an analogous helical peptide, the Δ^ZPhe transition moments were theoretically predicted to lie approximately on a $C^\gamma-C^\alpha$ line (roughly, in the direction of the phenyl group to the helical main chain).[6a]

(20) For instance, see: (a) Usatyi, A. F.; Shlyakhtenko, L. S. *Biopolymers* **1973**, *12*, 45−51. (b) Richardson, J. M.; Makhatadze, G. I. *J. Mol. Biol.* **2004**, *335*, 1029−1037.

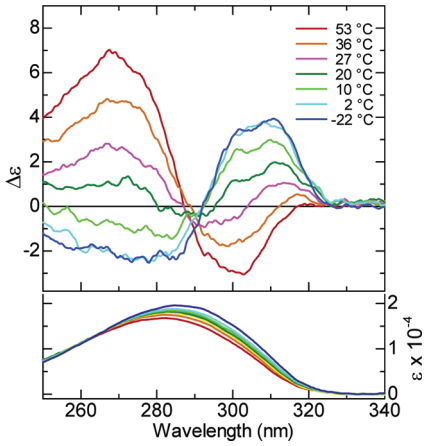

FIGURE 3. CD (upper) and UV absorption spectra of peptide **1** with Boc-D-Pro-OH in chloroform at temperatures ranging from −22 to 53 °C: [**1**] = 0.14 mM; [Boc-D-Pro-OH] = 1 mM

a weak, complicated CD pattern at 20 °C, not inducing a clear bias to a one-handed helix (Figure 3).[21]

Cooling of the solution, however, emerged a marked split-type pattern with a positive peak (at longer wavelengths) to a negative peak, (+ to −). Obviously, the temperature depression leads to the occurrence of a left-handed helix. This behavior is completely opposite to the case of only peptide **1** whose original right-handed helix is modestly stabilized by decreasing temperature. Thus, the external chiral effect at low temperature overcomes the internal effect to favor the opposite helix sense. Conversely, the heating from room temperature recovered the original CD signs for a right-handed helix.

The helix inversion through the cooling−heating process is not responsible for the thermodynamic difference between the two helices of peptide **1** itself. Clearly, the synergistic effect of chiral stimulus and temperature gives rise to the helix inversion. A similar temperature-driven control of helix sense was observed for a solution of **1** with a moderate amount of Boc-D-Leu-OH (1 mM), as shown in Figure 4. That is, the cooling below 28 °C induced a left-handed helix from a screw-sense balance, whereas the heating recovered the original right-handed helix.

The optically inactive 3_{10}-helical peptide **2** [H-β-Ala-(Δ^ZPhe-Aib)$_4$-OCH$_3$][6a,b] is capable of three-point interactions between the N-terminal sequence and the chiral Boc-amino acid (Pro or Leu)[6a] or Boc-Leu$_2$-OH.[6b] A similar interaction manner is also proposed in peptides N-capped by Gly and N-methyl Gly.[5c,6c] That is, the two hydrogen bonds and one ionic interaction occur upon its N-terminal sequence, cooperatively binding a Boc-amino acid molecule to make the starting point for the NCDE. Such hydrogen-bonding interactions, in general, become more stable at low temperature.[22] Thus, the external chiral power to operate on the first domino segment should be increased by decreasing temperature, whereas the degree of interaction reduces at high temperature. Consequently, the temperature effect modulates the Boc-amino acid−peptide affinity to determine the whole helix sense.

(21) In ref 7, a reversed CD pattern began to appear at 1 mM of Boc-D-Pro-OH. This inconsistency might be partly related to nonregulation of temperature in the previous condition, or to high sensitivity to CD pattern in this concentration region that almost produces a balance between the two helices.

(22) Dougherty, R. C. *J. Chem. Phys.* **1998**, *109*, 7372−7378.

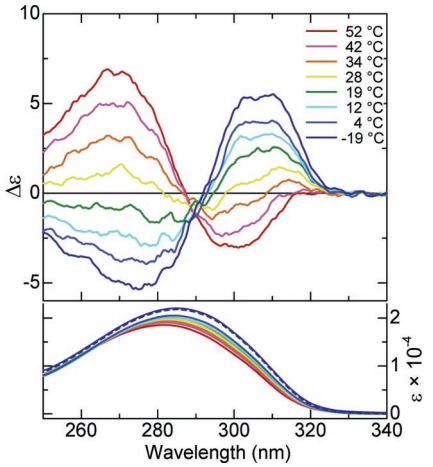

FIGURE 4. CD (upper) and UV absorption spectra of peptide **1** with Boc-D-Leu-OH in chloroform at temperatures ranging from −19 to +52 °C: [**1**] = 0.14 mM; [Boc-D-Leu-OH] = 1 mM. The UV absorption spectrum at −19 °C was also expressed through baseline correction (blue dashed line): see the Experimental Section.

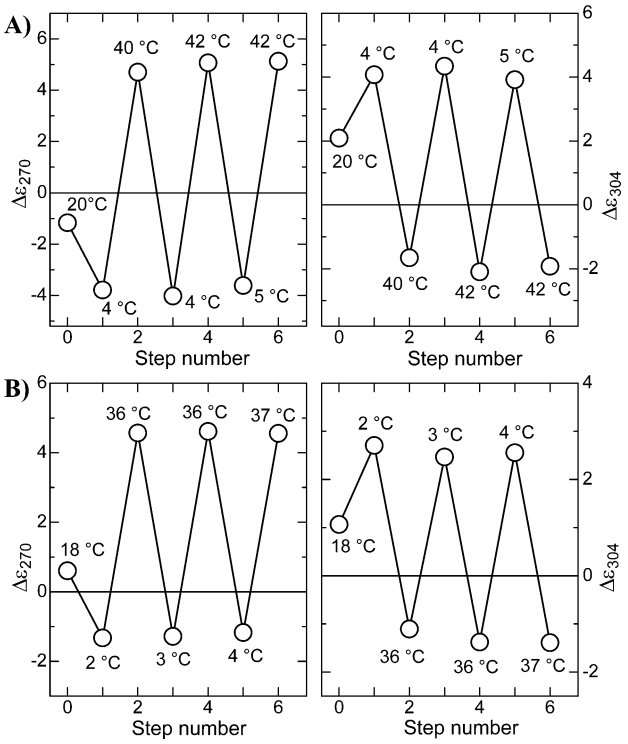

FIGURE 5. Temperature-induced chiroptical switching in a chloroform solution of peptide **1** with (A) Boc-D-Leu-OH or (B) Boc-D-Pro-OH: [**1**] = 0.14 mM; [Boc-amino acid] = 1 mM. Each solution started from room temperature to cooling−heating cycles: each temperature value is indicated near the corresponding plot.

Figure 5 displays the thermal history in CD values of peptide **1** with Boc-(D-Leu or D-Pro)-OH. Starting from room temperature, the cooling−heating cycles were repeated 2.5 times.

In the case of both Boc-amino acid additives, the inversion of the helix sense is substantially maintained in the temperature course. Thus, the phenomenon is defined as a thermodynamically reversible process originating from the terminal-specific temperature effect. Consequently, the temperature-driven switching of CD signs has been demonstrated in NCDE-based control

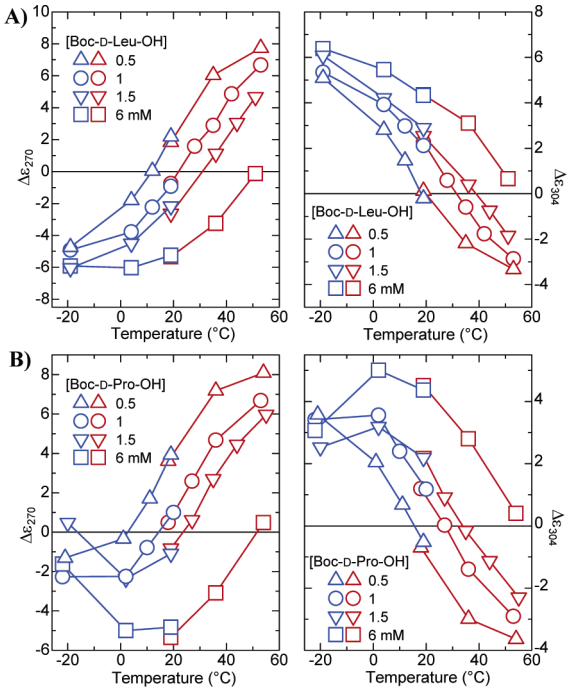

FIGURE 6. Temperature dependence of CD values of peptide **1** with (A) Boc-D-Leu-OH and (B) Boc-D-Pro-OH in chloroform: [**1**] = 0.14 mM; [Boc-amino acid] = 0.5, 1, 1.5, and 6 mM. For a given solution, its temperature changed from ca. 20 °C to a lower temperature (blue) or to a higher temperature (red).

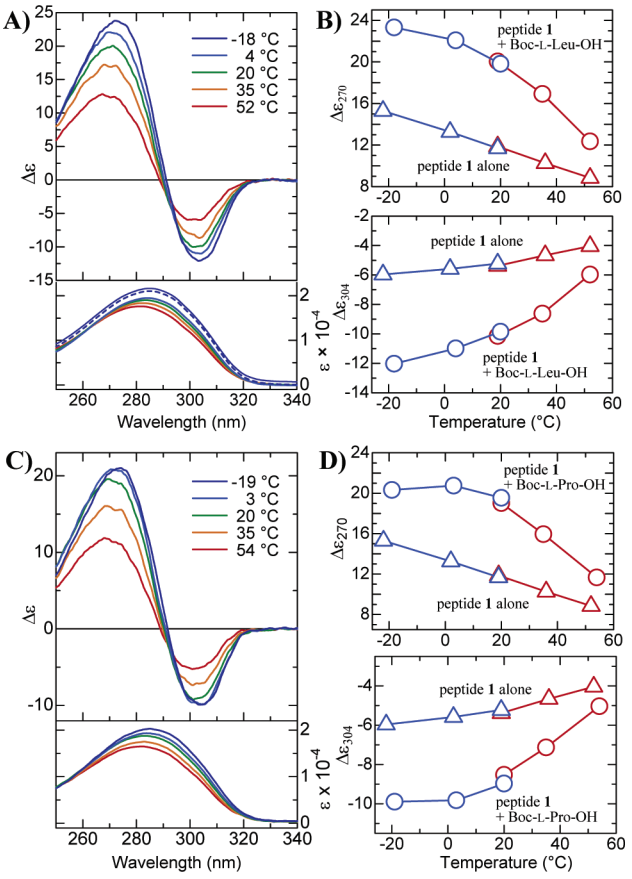

FIGURE 7. (A) CD (upper) and UV absorption spectra of peptide **1** with Boc-L-Leu-OH in chloroform at various temperatures. (B) Temperature dependence on CD values of peptide **1** with and without Boc-L-Leu-OH. For the corresponding figures for Boc-L-Pro-OH, see (C) and (D): [**1**] = 0.14 mM; [Boc-L-amino acid] = 1 mM. In (B) and (D), the data of peptide **1** alone were basically taken from Figure 2. For a given solution, its temperature changed from ca. 20 °C to a lower temperature (blue) or to a higher temperature (red). In (A), the UV absorption spectrum at −18 °C was also expressed through baseline correction (blue dashed line): see the Experimental Section.

of peptide helicity, whereas stimuli-induced chiroptical switches have been found in a wide variety of molecular systems.[4]

Effects of Chiral Stimulus and Temperature on Helix Sense. To evaluate the contribution of chiral/temperature factors simultaneously, a similar CD experiment was carried out with respect to different amounts of Boc-D-Leu-OH. Figure 6 summarizes the plots of $\Delta\epsilon$ value against solution temperature. The D-isomer at 0.5 and 1.5 mM brought about temperature-induced inversion of the helix, similar to the case of 1 mM. The thermal effect for the helix−helix transition keeps active at these concentrations. In contrast, the helix inversion was not clearly observed for a larger excess of Boc-D-Leu-OH (6 mM: it is around a saturation point where CD signals for a left-handed helix are induced at room temperature[7]), although a screw-sense balance from the left-handed helix was seen at 51 °C. Similar phenomena were found in peptide **1** with Boc-D-Pro-OH at the same concentrations (0.5, 1, 1.5, and 6 mM).

Figure 6 demonstrates that the peptide helix sense is sensitive to both effects of chiral stimulus and temperature. An increase in the initial concentration of the chiral additive promotes the chance that the chiral molecule encounters the N-terminal segment to facilitate the helix inversion. Conversely, temperature elevation weakens the external chiral power. Therefore, a simultaneous increase in the concentration and temperature produces the opposite effect on the induced helix sense. In other words, the helix inversion should be mainly derived from the tuning of the two external stimuli governing the NCDE.

In the case of Boc-D-Pro-OH (especially at 1.5 and 6 mM), the CD intensities of a left-handed helix decreased unexpectedly at about −20 °C (Figure 6B). In contrast, such a decrease was not essentially observed in the case of Boc-D-Leu-OH at −19 °C. Although we cannot explain the difference for now, the current system implies that a subtle difference in complexation manner at the N-terminus reflects the resulting CD signals based on the ratio of two helical contents.

Temperature Effect on Helicity of Peptide 1 with Boc-L-Amino Acid. We also have focused on the case of the corresponding Boc-L-amino acid that was shown to promote the original right-handed helix.[7] Figure 7A shows CD spectra and their amplitudes of **1** with Boc-L-Leu-OH at several temperatures. A variation ranging from −18 to +52 °C maintained the helix sense at room temperature, while the cooling increased the original CD amplitude. It is obvious that the temperature variation produces the opposite sense with respect to the chiral sign of Boc-Leu-OH.

Figure 7B indicates that the original helicity of peptide **1** with the L-isomer is promoted by cooling, similar to the case of only peptide **1**. However, the CD amplitudes of **1** with the L-isomer exceed those without the L-isomer, thus supporting that both effects, the L-isomer and temperature, are active.

On the other hand, the two CD values, with and without Boc-L-amino acid, approached each other above 35 °C, then coming closer at around 52 °C. This suggests that the thermal stimuli above about 35 °C begin to reduce the external chiral effect. In other words, Boc-L-Leu-OH showed stronger dependence of temperature on CD intensity around 20−52 °C than the case of

only peptide **1** (Figure 7B). Thus, the promotion of helicity by the L-isomer and temperature is suggested, as illustrated in Figure 1B.

In contrast, the CD intensity did not increase largely below room temperature, whereas the corresponding D-isomer led to a dramatic change of CD spectra at low temperature. A similar tendency was seen in the Boc-L-Pro-OH additive (Figure 7D), where the right-handed helicity at room temperature was not essentially promoted by decreasing temperature. Presumably, the right-handed helix assisted by these L-isomers should be fully stabilized around room temperature, thus not causing a significant increase in the CD signals at low temperature.

Influence of Peptide Concentration on Temperature-Driven Control of Helix Sense. We have proposed the NCDE model for control of the helix sense of a single peptide chain, as depicted in Figure 1 (or Table of Content graphic) as well as in refs 5−7. On the other hand, the actual experiment might be accompanied with some aggregation between peptide molecules. As a hydrophobic peptide often undergoes self-aggregation in organic solvent,[23,24] peptide **1** in chloroform should be prone to form some aggregates.[25]

To investigate the influence of self-aggregation on the thermal control, we have chosen two concentrations of **1**, around 2.6 mM and 7 μM. The latter is about 20 times as dilute as in the preceding condition (around 0.14 mM) that still suggests some self-aggregation.[26] The former is close to that used for NMR spectroscopy of peptide **1** versus chiral Boc-Leu-OH (as shown later). These CD results are shown in Figures S1−S6.

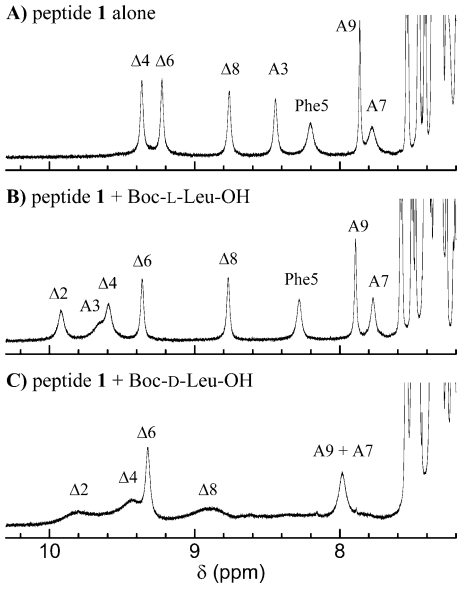

FIGURE 8. Influence of chiral additive on ^{1}H NMR (600 MHz) spectra of peptide **1** in $CDCl_3$ at 293 K: (A) **1** alone; (B) with Boc-L-Leu-OH; (C) with Boc-D-Leu-OH: [**1**] = ca. 2.7 mM; [Boc-Leu-OH]/[**1**] = ca. 2.3. The expanded region focuses mainly on amide NH resonances of **1**. Δ and A indicate Δ^ZPhe and Aib, respectively, where the following number is the residue number from the N-terminal β-Ala(1).

In summary, similar temperature effect on the helix sense was observed in the different concentrations (around 2.6 mM, 0.14 mM, and 7 μM), although such a wide concentration range, more or less, should affect peptide aggregation. In other words, the present aggregation does not disturb the control of helix sense, which should originate from the steady interaction mode of the helical peptide−chiral molecule.

NMR Study for Evidence of the NCDE. The model proposed in Figure 1 is based on the external chiral molecule interacting with the N-terminal sequence to initiate the NCDE. (Although the chiral molecule encounters the whole helical chain, chiral interaction at the terminus plays a key for control of the helicity.) The NCDE mechanism has been experimentally proposed in optically inactive peptides.[6] Their N-terminal segment of 3_{10}-helix inherently involves three functionalities (the amino and two amide NHs)[6] to participate in complementary binding to a chiral Boc-amino acid molecule for the helix-sense induction.[27]

We have not so far obtained experimental data for direct evidence of the N-terminal complexation in the present system. Correspondingly, NMR studies have been carried out for a solution of **1**−Boc-amino acid. Figure 8 displays 1D-NMR spectra of **1** without and with Boc-Leu-OH at room temperature.[26] In contrast to the absence of chiral additive, peptide **1** with Boc-L-Leu-OH offered two striking changes in amide NH chemical shifts. First, the NH peak of Aib(3) (third from the N-terminus) remarkably moved to a low magnetic field. Second,

(23) For instance, see: (a) Iqbal, M.; Balaram, P. *Biopolymers* **1982**, *21*, 1427−1433. (b) Iqbal, M.; Balaram, P. *Biochemistry* **1981**, *20*, 7278−7284. (b) Raj, P. A.; Balaram, P. *Biopolymers* **1985**, *24*, 1131−1146. (c) Toniolo, C.; Bonora, G. M.; Marchiori, F.; Borin, G. *J. Am. Chem. Soc.* **1984**, *106*, 1455−1457. (d) Ganesh, S.; Jayakumar, R. *J. Pept. Res.* **2003**, *61*, 122−128.

(24) (a) Sakamoto, R.; Watanabe, M. *Contemp. Top. Polym. Sci.* **1984**, *4*, 259−268. (b) Weill, G.; André, J. J. *Biopolymers* **1978**, *17*, 811−814. (c) Gupta, A. K.; Dufour, C.; Marchal, E. *Biopolymers* **1974**, *13*, 1293−1308. (d) Wada, A. *J. Polym. Sci.* **1960**, *45*, 145−154. (e) Gupta, A. K. *Biopolymers* **1976**, *15*, 1543−1554. (f) Sisido, M.; Shimizu, T.; Imanishi, Y.; Higashimura, T. *Biopolymers* **1980**, *19*, 701−711.

(25) We encountered inexplicable phenomena when investigating dependence of the concentration of **1** on the ^{1}H NMR spectra in $CDCl_3$. In the case of [**1**] = 2 or 2.7 mM, relatively well-resolved resonances were seen for seven amide NH's [Aib(3) to Aib(9)] and C-terminal methoxy group. However, decreasing concentration yielded a more complicated pattern. In particular, the methoxy resonance appeared to be divided into three peaks or more at [**1**] = 0.14 mM, around which the preceding CD studies were carried out. Thus, the CD results in Figures 2−7 might contain some self-aggregation factors. Incidentally, in the dilution process, a peptide solution often became turbid. Presumably, some self-aggregation modes might be gradually changed from one to another by the dilution. As for hydrophobic helical peptides, "head-to-tail" and "side-by-side" have been proposed for their aggregation modes.[11b,24]

(26) As described in ref 25, peptide **1** should be considered to participate in self-aggregation. This aggregated species should offer diverse magnetic environments to generate a more complicated pattern. Under such a situation, we hardly focus on the nature of a single peptide chain. However, a relatively high concentration of peptide **1** (around 2.7 mM: usually chosen for the present NMR study) yielded a relatively simple pattern. That is, seven NH resonances of the Aib(3) to Aib(9) residues as well as the C-terminal methoxy resonance appeared essentially as a single peak at 293 K (Figure S8). A similar tendency was seen in the presence of Boc-L-Leu-OH. (In comparison of Figures S8 and S9, the methoxy proton of only **1** shifted to a higher magnetic field.) Fortunately, the condition used in Figures 8 and 9 does not lead to undesirable spectral damages by self-aggregation. It can provide a good scope for analysis of the local conformation and the complexation manner. Thus, the distorted NMR pattern of peptide **1**−Boc-D-Leu-OH (Figure 8C) should reflect local conformations differing in magnetic environments, because it was obtained in a condition similar to the preceding case of Boc-L-Leu-OH. This interpretation might also be supported from Figure S10, where the terminal methoxy proton of peptide **1** with the D-isomer appears as an essential single peak.

(27) Free amide groups that originally appear in terminal sequences of peptide or protein helices are prone to interact with other hydrogen-bonding parts. For elegant examples relating to helical terminal motifs, see: (a) Baldwin, R. L.; Rose, G. D. *Trends Biochem. Sci.* **1999**, *24*, 26−33. (b) Richardson, J. S.; Richardson, D. C. *Science* **1988**, *240*, 1648−1652. (c) Cochran, D. A. E.; Penel, S.; Doig, A. *J. Protein Sci.* **2001**, *10*, 463−470. (d) Harper, E. T.; Rose, G. D. *Biochemistry* **1993**, *32*, 7605−7609. (e) Petukhov, M.; Yumoto, N.; Murase, S.; Onmura, R.; Yoshikawa, S. *Biochemistry* **1996**, *35*, 387−397. (f) Seale, J. W.; Srinivasan, R.; Rose, G. D. *Protein Sci.* **1994**, *3*, 1741−1745.

the L-additive clearly emerged the Δ^ZPhe(2) NH resonance, which was not markedly observed at 293 K in peptide **1** alone. In comparison with the Aib(3) NH resonance, the remaining Δ^ZPhe(4) to Aib(9) NH's were relatively sensitive to the L-additive.

Hence, the six NH groups are basically shielded from the chiral additive, supporting that the original hydrogen-bonding pattern of 3_{10}-helix[6,7] should be essentially maintained in the complex formation. The large changes in the Δ^ZPhe(2) and Aib(3) NH resonances should be attributed to a hydrogen-bond with two carbonyl acceptors of Boc-L-Leu-OH.[6,7] In other words, the chiral molecule binds the N-terminal segment of H-β-Ala-Δ^ZPhe-Aib-, whereas the remaining part should be virtually inert for its chiral binding or recognition.

Similar NMR spectral changes were found in achiral peptide **2** or N-Gly capped peptide versus N-blocked amino acid.[6] Thus, the complexation manner proposed in refs 6a,c should be applied to the present case. The N-amino group and carboxylic acid tend to undergo ionic interaction.[28] Two hydrogen bonds form in the Δ^ZPhe(2) NH−Boc carbonyl and the Aib(3) NH−carboxylate oxygen. The three-point binding on the H-β-Ala-Δ^ZPhe-Aib- fragment was theoretically proven in refs 6a,29.

On the other hand, Boc-D-Leu-OH yielded a more complicated profile, in which most of the signals were broadening or deformed. As shown in the preceding CD studies, the D-isomer reduces the original screw-sense bias to induce an opposite helix, whereas the corresponding L-isomer tends to promote the original right-handed helix. The chiral additive-induced CD intensity indicated that a bias to a one-handed helix is much smaller in the D-isomer. Thus, the D-additive will permit two left-handed/right-handed helices in equilibrium.

Dynamic conversion between two molecular forms is often accompanied with line broadening of NMR signals when the conversion rate is comparable to the spectroscopic time scale.[30] Thus, the signal broadening in Figure 8C suggests dynamic conversion between the two helices. In the NMR spectroscopy, temperature as a scaling factor can control the conversion rate.[30a] If such a helix−helix transition occurs, decreasing temperature splits a broadening signal into two.[30]

Correspondingly, NMR spectra of peptide **1** at 273 K are shown in Figure 9. Boc-D-Leu-OH (Figure 9C) produced a complicated pattern but a relatively clear separation of each signal. Signal resolution improved at low temperature, and the apparent number (ca. 12−13) of the signals detectable as amide NHs support our speculation. Thus the D-isomer allows the two helical conformations to be present as comparable populations in equilibrium. In contrast, peptide **1** with Boc-L-Leu-OH at 273 K (Figure 9B) showed, at a lower magnetic field, relatively clear eight signals that should be assigned to all the amide NHs. Apparently, a one-handed helix (right-handed sense identified from the CD results) is essentially predominant in the presence of the L-isomer, which renders the other helix unstable.

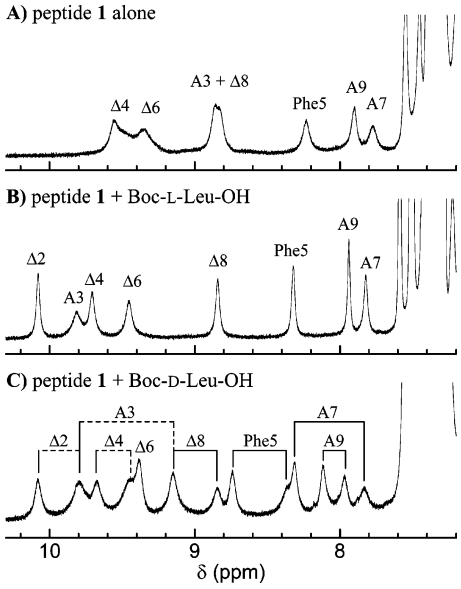

FIGURE 9. Low-temperature ^{1}H NMR spectra of (A) peptide **1** alone and that with (B) Boc-L-Leu-OH or (C) Boc-D-Leu-OH in $CDCl_3$ at 273 K. For 293 K, see Figure 8. For the assignment of amide NHs, see the Experimental Section. The NH assignment in (C) is tentative due to its crowded pattern.

Therefore, the NMR changes induced by external chiral stimulus are fully consistent with the previous conclusion driven from CD study: that is, the L-isomer produces a predominantly right-handed helix, whereas the D-isomer induces an equilibrium state biased toward a left-handed helix.[7,31] As for Figures 8 and 9, more detailed changes are given in the Supporting Information.

The corresponding NOESY spectra were acquired for further information on complex structure. As shown in Figure 10, the combination of peptide **1** and Boc-L-Leu-OH yielded two NOE signals attributed to correlation of the Leu C$^\alpha$H with the Δ^Z-Phe(2) NH or Aib(3) NH. In contrast, distinct cross-peaks between the C$^\alpha$H and the other amide NH's [Δ^ZPhe(4) to Aib(9)] were not found in the current condition.[32] Obviously, spatial proximities between the two proton pairs noticed above are accompanied with the dynamic complexation. The NOE observation proves that the L-isomer is dynamically localized at the N-terminal sequence for initiation of the NCDE.

In the case of Boc-D-Leu-OH (Figure 11), two intermolecular NOE signals, though relatively small, were observed between C$^\alpha$H (Leu) and amide NH resonances at a low magnetic region.

Among the two correlated NHs, one appearing more downfield is assignable to one of the split Δ^ZPhe(2)'s. The other intermolecular NOE is hardly identified due to overlap between two signals, which might be assigned to the other Δ^ZPhe(2) or one of the two Aib(3) signals. However, we can claim at least

(28) Acid−base interaction in apolar solvent is deeply discussed in refs 28a,b: (a) Yashima, E.; Matsushima, T.; Okamoto, Y. *J. Am. Chem. Soc.* **1997**, *119*, 6345−6359. (b) Takenaka, S.; Kondo, K.; Tokura, N. *J. Chem. Soc., Perkin Trans. 2* **1975**, 1520−1524.

(29) Inai, Y.; Ousaka, N.; Miwa, Y. *Polym. J.* **2006**, *38*, 432−441.

(30) (a) Kessler, H. *Angew. Chem., Int. Ed.* **1970**, *9*, 219−235. (b) Hummel, R.-P.; Toniolo, C.; Jung, G. *Angew. Chem., Int. Ed.* **1987**, *26*, 1150−1152. For dynamic helix−helix transition in NMR method, refs 3a,b; see also: (c) Ute, K.; Fukunishi, Y.; Jha, S. K.; Cheon, K.-S.; Muñoz, B.; Hatada, K.; Green, M. M. *Macromolecules* **1999**, *32*, 1304−1307. (d) Scaglioni, L.; Mazzini, S.; Mondelli, R.; Merlini, L.; Ragg, E.; Nasini, G. *J. Chem. Soc., Perkin Trans. 2* **2001**, 2276−2286.

(31) Assuming that the NH peaks in Figure 9C originate from the two helices, the intensity ratio of main (stronger)/second peaks for each of two-split NH resonances will suggest the population ratio ($R_{L/R}$) of left-handed helix (preferential)/right-handed helix. Its crowded pattern prevents us from a comprehensive, precise estimation of $R_{L/R}$. If the two peaks around 8.9−8.7 ppm (Figure 9C) are assigned to the second peak of Δ^ZPhe(8) and the main peak of Phe(5), the $R_{L/R}$ value might be estimated to be about 58/42.

(32) For the NOESY of a wide area, see the Supporting Information. Intermolecular NOEs other than the amide NH's were not clearly identified for now due to a complicated pattern at a high magnetic field, where alkyl protons of chiral additive as well as peptide **1** were partially overlapped. A similar situation should apply to intermolecular NOEs of achiral peptide **2** versus Boc-amino acid.[6a]

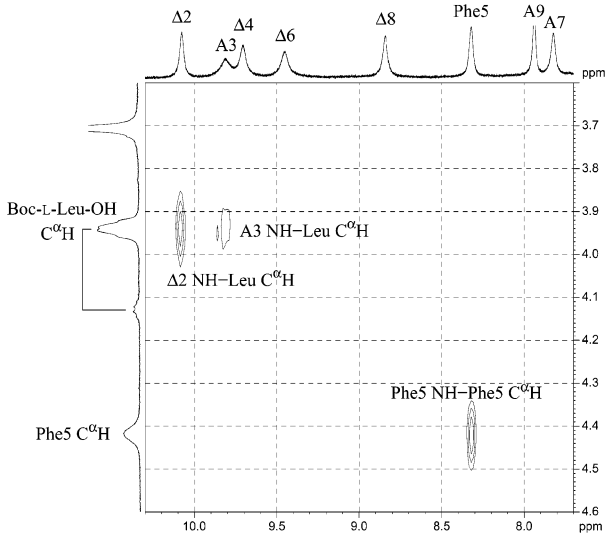

FIGURE 10. NOESY spectrum of peptide **1** with Boc-L-Leu-OH in $CDCl_3$ at 273 K: [**1**] = ca. 2.7 mM; [Boc-L-Leu-OH]/[**1**] = ca. 2.3. The area mainly focuses on amide NH's (**1**)−$C^{\alpha}H$'s [Boc-L-Leu-OH and Phe(5)]. A minor peak of Phe(5) $C^{\alpha}H$ might be present at around 4.1 ppm, according to cross-peaks in Figure S14A

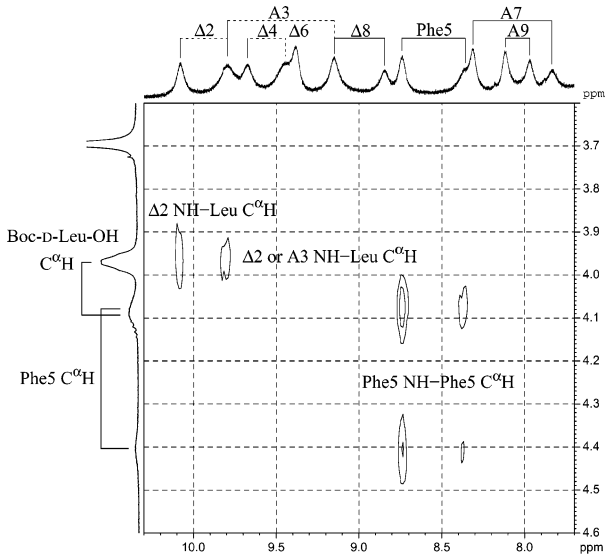

FIGURE 11. NOESY spectrum of peptide **1** with Boc-D-Leu-OH in $CDCl_3$ at 273 K: [**1**] = ca. 2.7 mM; [Boc-D-Leu-OH]/[**1**] = ca. 2.3. The area mainly focuses on NH's (**1**)−$C^{\alpha}H$'s [Boc-D-Leu-OH and Phe-(5)]. The assignment of NH and $C^{\alpha}H$ resonances, including their cross-peaks, was tentatively performed due to its crowded pattern.

that Boc-D-Leu-OH molecule in complex formation favors mainly the N-terminal sequence, likewise in the case of Boc-L-Leu-OH.

In Figure 9C, the peak-splitting behavior continued to the C-terminal sequence of -Aib(7)-Δ^{Z}Phe(8)-Aib(9)-OCH_3. This implies that chiral signal received at the N-terminal sequence influences conformations of the whole backbone as proposed in Figure 1.[5,6]

Comparison with Other Models for Thermal-Driven Control of Helix Sense. Several leading studies concerned with the present model have been reported. First, the preferential generation of a one-handed helix through chiral moiety at the chain terminus has been demonstrated in unique systems, where a chemically chiral unit is covalently linked to the terminal position of an optically inactive chain.[33] These helical models might be defined as the covalent chiral domino effect (CCDE).[5b,e,6a,33] When the CCDE-induced helix sense is affected by temperature effect, some conformational changes about the chiral terminus might largely influence a helix sense in the remaining achiral segment.[33] Thermal tuning of noncovalent chiral interactions governing control of helicity has been elegantly demonstrated by Yashima and co-workers.[34] Regarding site-specific chiral induction, the elegant system has been proposed that chiral duplex is induced between complementary "peptide nucleic acid" chains containing a chiral residue at the terminal position.[35] In addition, a polymeric chain of nucleic acids undergoes helix-to-helix transition depending on environmental changes such as salt addition and temperature variation.[3j−l]

In contrast to these leading systems, the model proposed in Figure 1 employs temperature as a modulator of the noncovalent chiral interaction. In the domino-type control, the helix sense of a target peptide can be manipulated with some optional stimuli specific to the first domino sequence.[6]

Figure 6 demonstrates that an increase in the concentration of external chiral molecule brings about elevation of switching temperature (T_S) of CD signs relating to the helix inversion. Recently, Green and co-workers[2a,b] have proposed a comprehensive, elegant principle, "chiral conflict",[2b] for designing a polymer chain enabling helix-sense inversion at such a desirable T_S value, in which two kinds of dissimilar monomer units with opposite chirality are covalently incorporated into a single chain to modulate thermodynamic parameters for helix inversion.[2a,b] From the thermodynamic viewpoint, the present helix inversion might be categorized into their principle.

On the other hand, our current model deals with temperature-mediated competition between noncovalent and covalent powers

(33) Similar references of CCDE are also given in ref 6: (a) Okamoto, Y.; Matsuda, M.; Nakano, T.; Yashima, E. *Polym. J.* **1993**, *25*, 391−396. (b) Obata, K.; Kabuto, C.; Kira, M. *J. Am. Chem. Soc.* **1997**, *119*, 11345−11346. (c) Obata, K.; Kira, M. *Macromolecules* **1998**, *31*, 4666−4668. (d) Maeda, K.; Okamoto, Y. *Polym. J.* **1998**, *30*, 100−105. (e) Mizutani, T.; Yagi, S.; Morinaga, T.; Nomura, T.; Takagishi, T.; Kitagawa, S.; Ogoshi, H. *J. Am. Chem. Soc.* **1999**, *121*, 754−759. (f) Mazaleyrat, J.-P.; Wright, K.; Gaucher, A.; Toulemonde, N.; Wakselman, M.; Oancea, S.; Peggion, C.; Formaggio, F.; Setnicka, V.; Keiderling, T. A.; Toniolo, C. *J. Am. Chem. Soc.* **2004**, *126*, 12874−12879. (g) Benedetti, E.; Saviano, M.; Iacovino, R.; Pedone, C.; Santini, A.; Crisma, M.; Formaggio, F.; Toniolo, C.; Broxterman, Q. B.; Kamphuis, J. *Biopolymers* **1998**, *46*, 433−443. (h) Toniolo, C.; Saviano, M.; Iacovino, R.; Crisma, M.; Formaggio, F.; Benedetti, E. *Z. Kristallogr.* **1999**, *214*, 160−166. (i) Crisma, M.; Valle, G.; Formaggio, F.; Toniolo, C. *Z. Kristallogr.* **1998**, *213*, 599−604. (j) Pengo, B.; Formaggio, F.; Crisma, M.; Toniolo, C.; Bonora, G. M.; Broxterman, Q. B.; Kamphuis, J.; Saviano, M.; Iacovino, R.; Rossi, F.; Benedetti, E. *J. Chem. Soc., Perkin Trans. 2* **1998**, 1651−1657. (k) Pieroni, O.; Fissi, A.; Pratesi, C.; Temussi, P. A.; Ciardelli, F. *J. Am. Chem. Soc.* **1991**, *113*, 6338−6340. (l) Tuzi, A.; Ciajolo, M. R.; Guarino, G.; Temussi, P. A.; Fissi, A.; Pieroni, O. *Biopolymers* **1993**, *33*, 1111−1121. (m) Pieroni, O.; Fissi, A.; Pratesi, C.; Temussi, P. A.; Ciardelli, F. *Biopolymers* **1993**, *33*, 1−10. (n) Inai, Y.; Ashitaka, S.; Hirabayashi, T. *Polym. J.* **1999**, *31*, 246−253. (o) Ousaka, N.; Inai, Y. *J. Am. Chem. Soc.* **2006**, *128*, 14736−14737. (p) For another unique model in the NCDE-type induction of a helix sense, see: Mizutani, T.; Sakai, N.; Yagi, S.; Takagishi, T.; Kitagawa, S.; Ogoshi, H. *J. Am. Chem. Soc.* **2000**, *122*, 748−749.

(34) (a) Morino, K.; Maeda, K.; Yashima, E. *Macromolecules* **2003**, *36*, 1480−1486. (b) Yashima, E.; Maeda, K.; Yamanaka, T. *J. Am. Chem. Soc.* **2000**, *122*, 7813−7814. For control of helicity by external chiral stimuli, see also: (c) Yashima, E.; Maeda, Y.; Okamoto, Y. *J. Am. Chem. Soc.* **1998**, *120*, 8895−8896.

(35) (a) Kozlov, I. A.; Orgel, L. E.; Nielsen, P. E. *Angew. Chem., Int. Ed.* **2000**, *39*, 4292−4295. (b) Wittung, P.; Eriksson, M.; Lyng, R.; Nielsen, P. E.; Nordén, B. *J. Am. Chem. Soc.* **1995**, *117*, 10167−10173. (c) Wittung, P.; Nielsen, P. E.; Buchardt, O.; Egholm, M.; Nordén, B. *Nature* **1994**, *368*, 561−563.

of single-point chiral information. The noncovalent chiral stimulus operates substantially on the N-terminal site of a helical chain. The control of helicity[5b,d,e,7,34] is based on external chiral power that is tuned by the mixing condition (selection of chiral additive and its concentration) or temperature.

Thermodynamics for Helix Inversion of the Current Model. Although the temperature-driven control of helix sense has been demonstrated, the scheme depicted in Figure 1 is oversimplified in contrast to the actual scheme. Finally, we discuss the current helix inversion from the viewpoint of thermodynamics.

When right-handed or left-handed helices (**RH** or **LH**) of **1** interact with Boc-D-amino acid (**D**) to yield complexes of **RH**−**D** or **LH**−**D**, the eqs 1−3 in equilibrium should be considered with definition of the corresponding free energies 4−6[36,37]

$$\mathbf{RH} \overset{K_{RL}}{\rightleftharpoons} \mathbf{LH} \tag{1}$$

$$\mathbf{RH} + \mathbf{D} \overset{K_{CR}}{\rightleftharpoons} \mathbf{RH}-\mathbf{D} \tag{2}$$

$$\mathbf{LH} + \mathbf{D} \overset{K_{CL}}{\rightleftharpoons} \mathbf{LH}-\mathbf{D} \tag{3}$$

$$\Delta\Delta G_{RL} = \Delta G_{LH} - \Delta G_{RH} \tag{4}$$

$$\Delta\Delta G_{CR} = \Delta G_{RH-D} - (\Delta G_{RH} + \Delta G_{D}) \tag{5}$$

$$\Delta\Delta G_{CL} = \Delta G_{LH-D} - (\Delta G_{LH} + \Delta G_{D}) \tag{6}$$

Here, K and ΔG mean equilibrium constant and free energy of each species, respectively. Conversion between **RH**−**D** and **LH**−**D** is not taken into account, because such helix−helix transition is suggested to occur more slowly than such exchange between one additive molecule and another.[6c] Self-aggregations of peptide **1** or the D-additive are also neglected for simplification (this treatment might support the view that temperature-mediated inversion of helix sense occurs regardless of the concentration of **1**). Equations 1−3 are formally expressed[36]

$$K_{RL} = [\mathbf{LH}]/[\mathbf{RH}] \tag{7}$$

$$K_{CR} = [\mathbf{RH}-\mathbf{D}]/([\mathbf{RH}]\cdot[\mathbf{D}]) \tag{8}$$

$$K_{CL} = [\mathbf{LH}-\mathbf{D}]/([\mathbf{LH}]\cdot[\mathbf{D}]) \tag{9}$$

A combination of eqs 7−9 gives

$$[\mathbf{LH}-\mathbf{D}]/[\mathbf{RH}-\mathbf{D}] = (K_{RL}\cdot K_{CL})/K_{CR} \tag{10}$$

Equations 7 and 10 are thermodynamically defined using eqs 4−6:[36]

$$\ln([\mathbf{LH}]/[\mathbf{RH}]) = -\Delta\Delta G_{RL}/RT = (\Delta G_{RH} - \Delta G_{LH})/RT \tag{11}$$

$$\ln([\mathbf{LH}-\mathbf{D}]/[\mathbf{RH}-\mathbf{D}]) = (-\Delta\Delta G_{RL} - \Delta\Delta G_{CL} + \Delta\Delta G_{CR})/RT = (\Delta G_{RH-D} - \Delta G_{LH-D})/RT \tag{12}$$

Equation 12 expresses the [**LH**−**D**]/[**RH**−**D**] ratio superficially on the basis of the equilibrium between **LH**−**D** and **RH**−**D**. That is, whichever the equilibrium is neglected or considered, the complex ratio is determined by using the energetic difference, not involving terms of other species.

Peptide **1** alone favors a right-handed helicity whose CD amplitude was increased by the cooling (Figure 2). Thus, [**LH**]/[**RH**] < 1 [that is, $(\Delta G_{RH} - \Delta G_{LH}) < 0$ in (11)] must be maintained in the temperature range studied. Accordingly, the fact that cooling of the **1**−**D** mixture induces an excess of a left-handed helical species cannot be attributed to a helical preference in **1** alone. Rather, it originates from increasing populations of complex species. In other words, [**LH**−**D**]/[**RH**−**D**] > 1 must occur at low temperature: that is, $(\Delta G_{RH-D} - \Delta G_{LH-D}) > 0$ in eq 12 is maintained in the induction of a left-handed helix. Consequently, the helix inversion is derived from a temperature-variable ratio of complex/noncomplex species and thermodynamic stability switched in the diastereomeric complexes. The significance of the diastereomeric pairing for the helix−helix transition has already been pointed out in the computational simulation.[7] That is, a similar trend in theoretical energy of each species was found: **LH**−**D** < **RH**−**D**, while **LH** > **RH**.[7] It should be noted that the thermodynamic treatment does not refer to structural dynamics at the molecular level for the domino-type control of helicity.

Conclusion

The domino-type control of a peptide helix is characterized by the view that chiral information at one terminus of its sequence spreads on the whole chain.[5−7,33] Such "terminal manipulation" to govern the NCDE can be addressed in several ways: chemical structure of chiral additive and the terminal sequence of a target helix (chemical combinations at the binding site); chiral additive's concentration; and environmental factors. Choice of chiral additive and the N-terminal sequence has been shown to be a first key.[5−7] Second stimuli such as solvent and temperature, coupled with the first effect, will modulate the helix sense and its bias. Temperature in the current NCDE system has been demonstrated to function as an efficient modulator of the external chiral stimulus. The findings will also offer design of peptide-based "chiroptical switches"[4] driven by the joint stimuli of temperature and chiral additive.

A terminal motif in protein helices is recognized as a key site for modulation of tertiary structures.[27] Here the free NHs appearing at the terminal sequence tend to form hydrogen bonds with side-chain groups to create a "capping box",[27d−f] which is often important for helix promotion or termination. In this regard, the NCDE implies the formation of a "noncovalent chiral capping box",[6c] thereby influencing structural asymmetry and stability in peptide helix. The present temperature effect influences formation of such a chiral capping box to modulate the helical stability.

(36) For general guidance in chemical equilibrium and its thermodynamics, see: Moore, W. J. *Physical Chemistry*, 4th ed.; Prentice Hall, Inc.: New Jersey, 1972; Chapter 8.

(37) For elegant examples of chiral binding schemes, see: (a) Prince, R. B.; Barnes, S. A.; Moore, J. S. *J. Am. Chem. Soc.* **2000**, *122*, 2758−2762. (b) Ishi-i, T.; Crego-Calama, M.; Timmerman, P.; Reinhoudt, D. N.; Shinkai, S. *J. Am. Chem. Soc.* **2002**, *124*, 14631−14641.(c) Borovkov, V. V.; Lintuluoto, J. M.; Sugeta, H.; Fujiki, M.; Arakawa, R.; Inoue, Y. *J. Am. Chem. Soc.* **2002**, *124*, 2993−3006.

Experimental Section

Materials. The preparation and characterization of peptide **1** were reported in ref 7. *N*-Boc-protected peptide **1** was passed through silica gel column in ethyl acetate; chloroform was used in the sample injection [a similar technique has been often applied to the author's (Y.I.) other works: solvent having high solubility for a target peptide has been used for its effective injection]. Basically, according to refs 6 and 7, the Boc group was deprotected with formic acid, followed by neutralization with $NaHCO_3$ solution to extract peptide **1** with chloroform. Peptide **1** was recovered through precipitation with chloroform/hexane (for general guidance of synthesis of peptide, see refs 38a,b; for formic acid-mediated deprotection of Boc group, see refs 38a,c).

CD Spectroscopy. CD and UV absorption data were obtained at the same time on a CD spectrometer used in ref 33o. An absorption spectrometer was also used to check peptide concentration. Sample solution was usually prepared at room temperature with distilled chloroform basically according to ref 7: ϵ_{max} per Δ^Z-Phe residue (around 280−285 nm) of **1** alone at room temperature was set to 1.8×10^4,[6a,12c] which corresponds to Figure 2 (19 °C) and Figure S1B (20 °C; a similar value of the ϵ_{max}/Δ^ZPhe unit was reported in ref 12b).

Temperature-regulated CD and UV absorption measurements were carried out by using a water-jacket type of cell holder through which appropriate liquid was circulated from a thermosetting bath. Here sample temperature was taken through direct immersion of a temperature sensor into the solution in a quartz cell with a path length of 1 mm ([**1**] = ca. 0.14 mM) or of 2 cm ([**1**] = ca. 7 μL: see Supporting Information). Temperatures monitored were uncorrected. For a higher concentration of **1** (ca. 2.6 mM: see the Supporting Information), another cell with a smaller path length was used; two quartz plates were spaced out by a spacer with an appropriate thickness (5×10^{-2} mm). Due to its thinness, a sensor could not be put into the solution. Instead, the solution temperature was indirectly estimated from the immersion of a sensor into a quartz cell (1 mm path length) containing solvent under a similar condition.

For a given solution, its temperature usually started at about 19−20 °C, then changing to a lower temperature or to a higher temperature. CD and UV absorption data were usually treated with appropriate mathematical smoothing on the equipped standard software. Simple baseline correction (parallel shift along the ordinate) was done for some low-temperature absorption spectra, whose its absorbance (around 350−360 nm) appeared upward possibly due to a frosted cell surface.

NMR Spectroscopy. ^{1}H NMR data were acquired on a 600 MHz spectrometer controlled by software, which was also used in refs 6b and 33o. The measurement was done typically in $CDCl_3$ at 293 or 273 K. (A desirable temperature (uncorrected) was automatically regulated.) Commercially available $CDCl_3$ was used without purification. NOESY spectra were obtained on the same spectrometer by using a standard pulse program,[39] basically with the following parameters: mixing time of 200 ms; 2048 data points in F2 with 4 or 8 scans; 256 points in F1. As an undesirable signal was observed at around 0 ppm, $CHCl_3$ resonance (ca. 7.26−7.27 ppm)[40] was used for the identification of tetramethylsilane (TMS). Chemical shift was finally calibrated with the TMS standard. Spectral analysis was basically performed with the NMR-equipped software or the SpinWorks[41] software. 2D-NOESY spectra were drawn in a similar manner to ref 6c.

NH Assignment in NMR Spectra. Assignment of amide NHs in peptide **1** at 293 K[42] was basically done with the NOESY $N_iH-N_{i+1}H$ cross-peaks (Figure S11), where seven singlets around 9.4−7.7 ppm were assigned to amide NH's.[43] The sequential assignment started with the Phe(5) NH identified from the NH−C$^\alpha$H correlation.[44] The fact that peptide **1** adopts a helical conformation[7] was also helpful for the discrimination between N-terminal and C-terminal sides: environmentally sensible NH's[7,14] should belong to the N-terminal sequence. One NH signal showed particularly strong dependence of temperature, compared with the other six peaks (see Figure S8 and ref 16). This tendency supports that the former proton is involved in the N-terminal sequence. This information and the NOESY-connectivity allows us to assign the most temperature-sensitive (or solvent-sensitive[7,14]) one to the Aib(3)'s NH and the other six to the Δ^ZPhe(4)−Aib(9)'s. The remaining NH, which is unclear at 293 K but seems to overlap with the Δ^Z-Phe(4) and Δ^ZPhe(6) NHs at 273 K (Figures 9A and S8), should be judged to be the Δ^ZPhe(2)'s.

The NH assignment at 273 K was made based on each NH peak at 293 to 273 K (Figure S8) and the NOESY at 273 K (Figure S13). In the presence of Boc-L-Leu-OH at 293 K, the amide NH's were identified from spectral changes with Boc-L-Leu-OH (Figure S7A) and the corresponding NOESY (Figure S12). The addition of Boc-L-Leu-OH induced a signal at about 9.8−9.9 ppm, which should be assigned to the remaining Δ^ZPhe(2) NH. The NH assignment at 273 K was done through each NH peak at 293 to 273 K (Figure S9) and the NOESY (Figure S14): the identification of Δ^ZPhe(2) NH was supported from NOESY correlation with β-Ala(1) CH_2.

Meanwhile, full assignment of the amide NH's of **1** with Boc-D-Leu-OH is considerably complicated, because the D-additive made most of NH signals broaden at 293 K (Figure S7B) to turn into crowded patterns at 273 K (Figure S10). Accordingly, the NH assignment at 273 K was tentatively done based on the NOESY spectrum (Figure S15). The information of the NH's positions of **1** with Boc-L-Leu-OH was preliminarily used here. In addition, some marked cross-peaks in the NOESY NH−NH region (Figure S15B) were assumed to appear as dynamic exchange[45] of identical protons in two states (left-handed and right-handed helices).

(38) (a) Izumiya, N.; Kato, T.; Aoyagi, H.; Waki, M. *Pepuchido Gosei no Kiso to Jikken (Principle and Practice of Peptide Synthesis*); Maruzen Co., Ltd.: Tokyo, Japan, 1985; SciFinder Scholar, American Chemical Society, CAN 103:37731. (b) Jones, J. *The Chemical Synthesis of Peptides*; Oxford University Press: New York, 1991. (c) Halpern, B.; Nitecki, D. E. *Tetrahedron Lett.* **1967**, *8*, 3031−3033.

(39) The pulse program was also used in ref 33o. For the pulse, see: Bodenhausen, G.; Kogler, H.; Ernst, R. R. *J. Magn. Reson.* **1984**, *58*, 370−388.

(40) (a) Tani, K.; Iseki, A.; Yamagata, T. *Angew. Chem., Int. Ed.* **1998**, *37*, 3381−3383. (b) Davies, M. W.; Wybrow, R. A. J.; Johnson, C. N.; Harrity, J. P. A. *Chem. Commun.* **2001**, 1558−1559.

(41) Marat, K. *SpinWorks*; University of Manitoba: Manitobe, Canada, 1999−2006 (http://www.umanitoba.ca/chemistry/nmr/spinworks/index.html).

(42) While the NH assignment was already made in a similar condition,[7] the detailed process was not described.

(43) We also referred to the fact that hydrogen-bonding NH of Δ^ZPhe residue often appears at a considerably low magnetic field.[9n] For comprehensive NMR methods about proton assignment and structural determination of biopolymers, see: (a) Wüthrich, K. *NMR of Proteins and Nucleic Acids*; John Wiley and Sons: New York, 1986. For NMR assignment for more general compounds, see: (b) Siverstein, R. M.; Webster, F. X. *Spectrometric identification of organic compounds*; John Wiley and Sons: New York, 1998; Chapter 4.

(44) A standard pulse program was used for proton correlation (also used in ref 33o). For the pulse, see: Bax, A.; Davis, D. G. *J. Magn. Reson.* **1985**, *65*, 355−360.

(45) For examples of exchange spectra for helical molecules, see refs 30c,d. For fundamental theory and method of NOESY exchange, see: Ernst, R. R.; Bodenhausen, G.; Wokaun, A. *Principles of Nuclear Magnetic Resonance in One and Two Dimensions*; Clarendon Press: Oxford, U.K., 1987; Chapter 9, pp 490−538.

Acknowledgment. We thank N. Ousaka for his technical assistance. This work was partially supported by the project (No. 16550142) of the Ministry of Education, Culture, Sports, Science, and Technology of Japan (MEXT) as well as the project (No. 12650883) for the initial motivation. The author (Y.I.) also thanks Tatematsu Foundation for partial financial support.

Supporting Information Available: Temperature-variable spectral data of peptide **1** at two additional concentrations with and without chiral Boc-Leu-OH; 1D and 2D NMR spectra of peptide **1** with and without chiral Boc-Leu-OH. This material is available free of charge via the Internet at http://pubs.acs.org.

JO0625305